Journal of Solid State Chemistry **163,** 319–324 (2002)
doi:10.1006/jssc.2001.9418, available online at http://www.idealibrary.com on IDEAL®

Synthesis and Crystal Structure of $Cs_2Nb_6Br_5F_{12}$: A Nb_6 Cluster Compound with a One-Dimensional $Nb_6Br^i_5F^i_7F^a_6$ Unit Connection

S. Cordier,[1] O. Hernandez, and C. Perrin

Laboratoire de Chimie du Solide et Inorganique Moléculaire, UMR 6511 CNRS-Université de Rennes 1, Institut de Chimie de Rennes, Campus de Beaulieu, Avenue du Général Leclerc, 35042 Rennes Cedex, France

Received July 18, 2001; in revised form September 20, 2001; accepted September 28, 2001

The synthesis and the crystal structure of $Cs_2Nb_6Br_5F_{12}$ containing octahedral niobium clusters are presented in this work. This bromofluoride is based on a $Nb_6L^i_{12}F^a_6$ (L = Br and F) unit and crystallizes in the orthorhombic system (space group, *Cccm*; $Z = 4$; $a = 9.2446(2)$ Å, $b = 13.6256(3)$ Å, and $c = 17.1665(4)$ Å; $R = 0.0241$). Fluorine and bromine are randomly distributed on the inner ligand positions, L^i, that edge-bridge the Nb_6 cluster whereas fluorine fully occupies the apical positions (L^a). The units are linked to each other by apical ligands leading to an original one-dimensional unit connection. The cesium atoms are statistically distributed on several sites that describe parallel channels along the [1 0 0] direction. The influence of fluorine ligands upon the stabilization of this structure type as well as the structural relationships with $Ba_2Zr_6Cl_{17}$(B), Nb_6F_{15}, and $NaMo_6Cl_{13}$ will be evidenced and discussed. © 2002 Elsevier Science

Key Words: **bromofluorides in niobium cluster chemistry; solid state synthesis; single-crystal X-ray diffraction; crystal structure.**

INTRODUCTION

In niobium cluster chemistry, numerous compounds have been reported with isolated Nb_6X_{18} units (X = Cl, Br) (1). Interconnections between units through apical ligands lead either to two- or to three-dimensional networks as observed in $Li_2Nb_6Cl_{16}$ (2), $NaNb_6Cl_{15}$ (3), and Nb_6F_{15} (4). According to the notation of Schäfer and Schnering (5), the Nb_6X_{18} units in the latter compounds are written $Nb_6Cl^i_{12}Cl^{a-a}_{4/2}Cl^a_2$, $Nb_6Cl^i_{12}Cl^{a-a}_{6/2}$, and $Nb_6F^i_{12}F^{a-a}_{6/2}$, respectively. While Nb–X^{a-a}–Nb intercluster bridges are bent for X = Cl or Br, they are always linear for X = F. Recently, we have entered the field of mixed halogen cluster compounds based on $Nb_6L^i_{12}L^a_6$ units with L = Cl/F or Br/F (6–9). Because of the large difference in their covalent radii and electronegativity, it turns out that the combined use of F and Cl or Br ligands allows us to modify the nanostructural and physical properties of the $Nb_6L^i_{12}L^a_6$ building blocks. Indeed, new structure types that cannot be isolated by using only one kind of halide have been stabilized, as illustrated by the examples of $Nb_6Br_8F_7$ and $Na_2Nb_7Br_4F_{17}$ (9). Both latter compounds are based on a $Nb_6L^i_{12}L^{a-a}_{6/2}$ unit network, but $Nb_6Br_8F_7$ exhibits bent bromine intercluster bridges, while $Na_2Nb_7Br_4F_{17}$ is characterized by linear fluorine intercluster bridges. We report herein the synthesis and structure of $Cs_2Nb_6Br_5F_{12}$ (orthorhombic system, space group *Cccm*; $Z = 4$) that is the first niobium cluster compound with a one-dimensional unit connection. The influence of fluorine ligand upon the stabilization of this structure type as well as the structural relationships with $Ba_2Zr_6Cl_{17}$(B) (10), Nb_6F_{15} (5), and $NaMo_6Cl_{13}$ (11, 12) will be evidenced and discussed.

SYNTHESIS

The title bromofluoride was first obtained as black microcrystals with an arrowhead-like shape during a preparation designed to obtain "$Cs_2Nb_7Br_4F_{17}$" that could have been isotypical to $Na_2Nb_7Br_4F_{17}$ (9). The compound was prepared by solid state reaction from a stoichiometric mixture of NbF_5 (Aldrich, 98%), $NbBr_5$ (Ventron, purity 99.998%), Nb powder (Ventron, m2N8), and CsBr (Merck, Pro Analysi). The starting powders were handled under an inert atmosphere. After grinding, the sample was formed as a pellet and introduced in a niobium container (Plansee) which was subsequently welded under argon and encapsulated in an evacuated silica ampoule. The final product was obtained as a black microcrystalline powder after 3 days of reaction, at a temperature equal to 800°C. Single crystals were always obtained on the inner side of the niobium tube. After a first structural resolution, the $Cs_2Nb_6Br_5F_{12}$ formula was obtained. Further syntheses were performed starting from different initial Br/F *ratios* in order to determine whether a phase breadth can be evidenced. Energy

[1]To whom correspondence should be addressed. stephane.cordier@univ-rennes1.fr.

0022-4596/02 $35.00

dispersive spectrometry (EDS) analyses, performed on several selected single crystals from each preparation, showed that they all contained the expected elements with a stoichiometry in agreement with that of the title compound. Furthermore, it turns out that the structural resolutions performed on single crystals from different preparations lead to the same refined stoichiometry—within the s.u.'s—whatever the starting composition. The powder X-ray diffraction patterns of samples belonging to the remaining pellet exhibit supplementary lines that could be attributed to Cs_2NbF_6 (13) and $CsNb_4Br_{11}$ (14). Their relative proportion depends on the initial Br/F *ratio*. In any case, the lines corresponding to the title compound were not shifted from one preparation to another, corroborating the fact that the phase breadth of $Cs_2Nb_6Br_5F_{12}$ is not significant.

STRUCTURAL DETERMINATION

The data collection has been carried out on a Nonius KappaCCD X-ray area detector diffractometer with Mo$K\alpha$ radiation ($\lambda = 0.71073$ Å). Details about the intensity measurement are reported in Table 1. $Cs_2Nb_6Br_5F_{12}$ crystallizes in the orthorhombic system, with a C-centered lattice. Once the data processing was performed by the KappaCCD analysis softwares (17–18), the cell parameters were refined to the following values: $a = 9.2446(2)$ Å, $b = 13.6256(3)$ Å and $c = 17.1665(4)$ Å. A multiscan absorption correction was performed through SORTAV (19). Among the possible space groups deduced from the observed systematic extinctions, the refinement procedure has allowed us to retain unambiguously the *Cccm* centrosymmetric space group. Direct methods (SIR97 program (20)) yielded a first partial structural solution, including the niobium cluster (constituted by the Nb1 and Nb2 atoms) and the fluorine apical ligands (F3 and F6 atoms). Subsequently, combined least-squares refinements and Fourier difference syntheses (CRYSTALS program (21)) allowed us to locate the inner ligands. After several cycles, it turned out that the $L1$ and $L2$ sites were not fully occupied by bromine, while the $L4$ and $L5$ sites were not fully occupied by fluorine, within the s.u.'s. Fluorine and bromine were then introduced with the same positional and thermal parameters as for bromine and fluorine on the $L1/L2$ and $L4/L5$ sites, respectively, but for each site the sum of the occupancies was restricted to the value corresponding to a fully occupied position. Afterward, the first two restraints were progressively relaxed during the convergence, leading to final positions in agreement with reliable Nb–(Br,F) interatomic distances. Due to its very low occupancy (0.017(3)), the Br4 atom has been refined with an isotropic displacement parameter. Once the unit of $Cs_2Nb_6Br_5F_{12}$ was refined, the Cs^+ countercations were located by Fourier difference syntheses. These atoms are disordered and five shared positions have been necessary to obtain a good agreement between observed and calculated structure factors (see Fig. 1). Moreover, the position of the F3 apical ligand is split because of the partial occupancy of the Cs1 site. Indeed, the Cs1 atom occupies only 69% of its site: as a consequence, the F3 apical fluorine is shifted from its position when the cesium site is empty. It results a statistical distribution of the F3 atom on three positions—refined with isotropic displacement parameters, the sum of the occupancies of these splitted sites being restricted to the value corresponding to a fully occupied position. Such a feature was not previously encountered since it is the first example of a compound with apical fluorine ligands that are not involved in intercluster bridges. The coordination number of the Cs atoms varies between 8 and 16 depending on the occupied position. The Cs–(Br,F) distances are within the range 1.994(9)–4.1745(1) Å. The cesium sites being statistically occupied, these distances correspond to an average between those observed locally for empty and full sites. Since the inner ligand sites are randomly occupied by fluorine and bromine and considering the discrepancy between their covalent radii (1.33 versus 1.82 Å (22), respectively), one would expect

TABLE 1
Single-Crystal Data Collection and Structure Refinement[a]

Chemical formula	$Cs_{2.1(2)}Nb_6Br_{4.73(4)}F_{12.27(4)}$
ρ_{calc} (g cm^{-3})	4.41
Crystal dimension (mm^3)	$0.11 \times 0.155 \times 0.135$
Temperature (K)	293
Crystal system	Orthorhombic
Space group	*Cccm*
Lattice constants (Å)	$a = 9.2446(2)$, $b = 13.6256(3)$, $c = 17.1665(4)$
Cell volume (Å^3)	2162.35(8)
Z	4
Range of data collection (°)	$1.00 < \theta < 34.97$
μ(Mo$K\alpha$) (mm^{-1})	15.2
Absorption correction	Multiscan (19)
Transmission factors	0.578 to 0.841
Total measured reflections	17,177
Unique reflections	2440
R_{int}	0.054
Observed reflections ($I > 3\sigma(I)$)	1602
R (observed reflections)	0.0241
R_w (observed reflections)	0.0248
S (goodness-of-fit)	1.08
Weighting scheme	Chebychev polynomial (23)
Variable parameters	131
Extinction coefficient	31 (2)
Max Δ/σ	0.0059
Difference Fourier map (e Å^{-3})	-0.98 to 0.98

Note. $R = \sum_{hkl}[||F_o| - |F_c||]/\sum_{hkl}[|F_o|]$; $R_w = \sqrt{\sum_{hkl}[w(i)(F_o - F_c)^2]}/\sqrt{\sum_{hkl}[w(i)F_o^2]}$; $S = \sqrt{\sum_{hkl}[w(i)(F_o - F_c)^2]/(m-n)}$ (m is the number of unique reflections, n the number of parameters). The refinement is done against F. Extinction correction: Eq. [22], Larson (24).

[a] A Nonius KappaCCD diffractometer was used for data collection (Mo tube, graphite monochromator); corrections for Lorentz and polarization effects were applied.

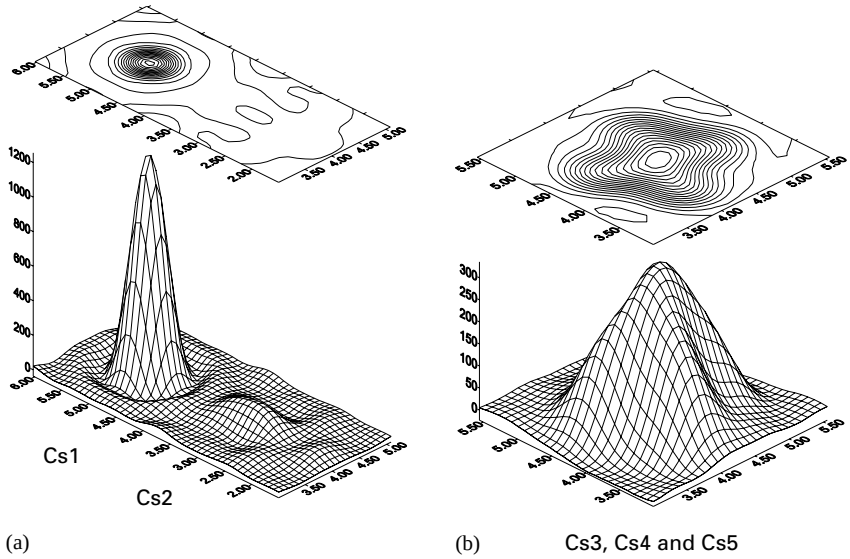

FIG. 1. Experimental electronic densities of the Cs atoms. The electronic densities, in e $Å^{-3}$ ($\times 10$), correspond to the observed structure factors: (a) in the (0 1 0) plane; (b) in the plane defined by Cs3, Cs4, and Cs5. The scale of the horizontal plane is defined in Å with an arbitrary origin.

that niobium atoms were subjected to a static disorder. The latter assumption is invalidated by the fact that the displacement parameters of niobium atoms do not display a significant shift from an isotropic atomic displacement and do not exhibit unusual values.

The final reliability factors are $R = 2.41\%$ and $R_w = 2.48\%$ (for 1602 $I > 3\sigma(I)$ observations versus 131 least-squares parameters). The final refinement leads to the following developed formula: $Cs_{2.1(2)}[Nb_6Br^i_{4.73(4)}F^i_{7.27(4)}]F^{a-a}_{2/2}F^a_4$. For clarity, we shall round the occupancies in order to obtain $Cs_2Nb_6Br_5F_{12}$. Details on the structure refinement parameters are reported in Table 1. The final atomic parameters and selected geometrical parameters are reported in Tables 2 and 3, respectively. Additional materials,

TABLE 2
Fractional Atomic Coordinates and Equivalent Isotropic Displacement Parameters ($Å^2$) for $Cs_2Nb_6Br_5F_{12}$

Atom	Wyckoff position	Site symmetry multiplicity	Refined multiplicity	x/a	y/b	z/c	U_{eq}
Nb1	16*m*	1		0.87085(3)	0.31476(2)	0.08147(1)	0.0169
Nb2	8l	0.5		0.62080(5)	0.36775(3)	0	0.0169
F1	16*m*	1	0.280(3)	1.005(1)	0.1945(6)	0.0892(5)	0.0261
Br1	16*m*	1	0.720(3)	1.07341(8)	0.18260(4)	0.10275(4)	0.0315
F2	8*k*	0.5	0.140(2)	$\frac{3}{4}$	$\frac{1}{4}$	0.1682(8)	0.0291
Br2	8*k*	0.5	0.360(2)	$\frac{3}{4}$	$\frac{1}{4}$	0.20959(5)	0.0273
F3	16*m*	1	0.23(9)	1.016(4)	0.392(2)	0.165(1)	0.014(5)
F31	16*m*	1	0.40(5)	0.982(2)	0.386(1)	0.1741(8)	0.023(2)
F32	16*m*	1	0.37(8)	0.997(2)	0.409(2)	0.1592(9)	0.019(3)
F4	16*m*	1	0.983(3)	0.7411(2)	0.4392(2)	0.0844(1)	0.0257
Br4	16*m*	1	0.017(3)	0.744(2)	0.486(2)	0.090(1)	0.022(7)
F5	8l	0.5	0.415(2)	0.9989(7)	0.3860(3)	0	0.0250
Br5	8l	0.5	0.085(2)	0.0653(5)	0.3973(3)	0	0.0271
F6	4c	0.25		$\frac{1}{2}$	$\frac{1}{2}$	0	0.0466
Cs1	4b	0.25	0.1724(6)	0	$\frac{1}{2}$	$\frac{1}{4}$	0.0187
Cs2	8g	0.5	0.084(1)	0.7968(4)	$\frac{1}{2}$	$\frac{1}{4}$	0.0648
Cs3	16*m*	1	0.12(3)	0.508(4)	0.523(6)	0.229(1)	0.1108
Cs4	4a	0.25	0.07(2)	$\frac{1}{2}$	$\frac{1}{2}$	$\frac{1}{4}$	0.0576
Cs5	16*m*	1	0.07(1)	0.009(2)	0.036(2)	0.2185(8)	0.0296

Note. Refined multiplicity = occupancy × (site symmetry multiplicity); $U_{eq} = 1/3\sum_i\sum_j(U^{ij}a^ia^j\mathbf{a}_i.\mathbf{a}_j)$, except for the F3, F31, F32, and Br4 atoms—refined isotropically—in which case the isotropic displacement parameters are given. Calculated formula, $Cs_{2.1(2)}[Nb_6Br^i_{4.73(4)}F^i_{7.27(4)}]F^{a-a}_{2/2}F^a_4$. Standard uncertainties are shown in parentheses.

TABLE 3
Selected Geometrical Parameters (Å) for $Cs_2Nb_6Br_5F_{12}$

Nb1–Nb1 × 2	2.7970(4)
Nb1–Nb1 × 2	2.8474(6)
Nb1–Nb2 × 4	2.8542(4)
Nb1–Nb2 × 4	2.7966(4)
Nb–L	
Nb1–F1	2.06(1)
Nb1–Br1	2.6237(8)
Nb1–F2	2.06(1)
Nb1–Br2	2.6198(7)
Nb1–F31	2.127(7)
Nb1–F32	2.189(8)
Nb1–F3	2.23(2)
Nb1–F4	2.077(4)
Nb1–Br4	2.61(4)
Nb1–F5	2.073(4)
Nb1–Br5	2.539(4)
Nb2–F1 × 2	2.11(1)
Nb2–Br1 × 2	2.6088(7)
Nb2–F4 × 2	2.070(2)
Nb2–Br4 × 2	2.50(3)
Nb2–F6 × 1	2.1199(4)

anisotropic displacement parameters, and observed and calculated structure factors can be obtained upon request from the authors.

RESULTS AND DISCUSSION

The structure of $Cs_2Nb_6Br_5F_{12}$ is based on $(Nb_6Br^i_5F^i_7)F^{a-a}_{2/2}F^a_4$ units (Fig. 2) that are interconnected through linear Nb–F^{a-a}–Nb bridges leading to infinite chains of units. Consequently, the unit network displays a one-dimensional character. These chains are arranged in such a way that they form parallel layers stacked perpendicularly to the *c*-axis. Within the layers, the chains spread along the $[\bar{1}\,1\,0]$ or $[1\,1\,0]$ direction, depending on whether they belong to a layer located at $z/c = 0$ or $\frac{1}{2}$ (Fig. 3). The chains of a given layer are related to those of the neighboring layers by a rotation of 111.7° with respect to the *c*-axis. The cohesion of the structure is achieved by cesium atoms lying within the interlayer space at $z/c = \frac{1}{4}$ and $\frac{3}{4}$. As stressed above, the cesium cations are disordered on several crystallographic positions, as previously observed for the counter-cations in $KNb_6Cl_{10}F_5$ (6), $CsNb_6Cl_8F_7$ (6), and $Na_2Nb_7Br_4F_{17}$ (9). This feature, which can be encountered in ordered halides (e.g., $NaNb_6Cl_{15}$ (3)), seems to be overemphasized whenever ligand sites are subjected to a random distribution, in particular when fluorine is involved. In the title compound, the positions statistically occupied by countercations describe parallel channels orientated along the [1 0 0] direction (Fig. 4).

In $Cs_2Nb_6Br_5F_{12}$, the Br and F atoms are randomly distributed on the edge-bridging cluster positions. The large difference between the covalent radii of these latter atoms combined with a large discrepancy of the F/Br *ratio* on the 12 inner ligand sites leads to a significantly distorted Nb_6 octahedron. Indeed, the Nb_6 cluster can be depicted as a $(Nb1)_4$ rectangle separating the two Nb2 atoms, inducing

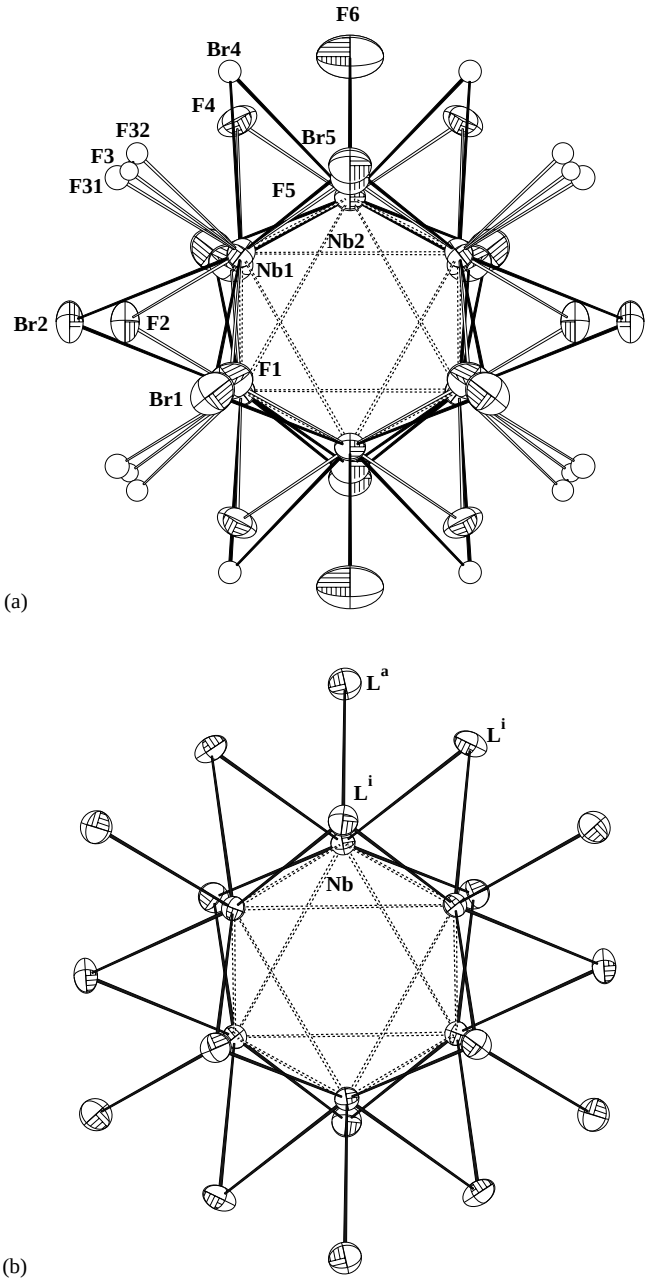

FIG. 2. (a) $(Nb_6Br^i_5F^i_7)F^{a-a}_{2/2}F^a_4$ unit. Displacement ellipsoids are shown at the 50% probability level. Only one of the two represented Br^i or F^i as well as the three F^a (F3, F31, F32) positions are locally occupied. The Nb–Nb, Nb–F, and Nb–Br bonds are represented by dashed, open, and filled black lines, respectively. (b) For the sake of comparison, projection of a standard $(Nb_6L^i_{12})L^a_6$ unit. The Nb–Nb and Nb–*L* bonds are represented by dashed and filled black lines, respectively.

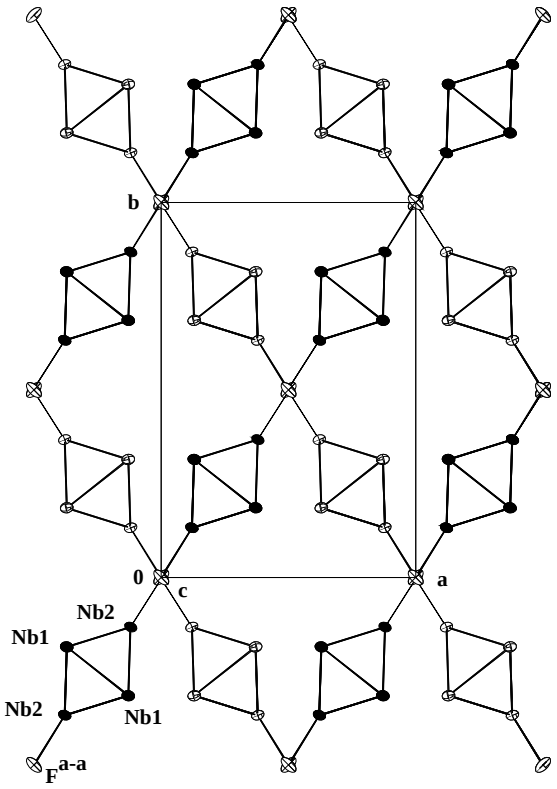

FIG. 3. Projection of the cluster chains along the [0 0 1] direction. The first layer at $z/c = 0$ is represented in gray whereas the second one at $z/c = \frac{1}{2}$ is represented in black. Displacement ellipsoids are shown at the 50% probability level. For the sake of clarity, only the Nb_6 clusters and the F^{a-a} ligands are represented.

a decrease of the cluster symmetry from $m\bar{3}m$ towards $2/m$, the angle between the normal of the $(Nb1)_4$ rectangle and the Nb2–Nb2 direction being equal to 1.6°. More specifically, the two Nb1–Nb1 bonds bridged by *L*2 are longer than the two others bridged by *L*5 (2.8474(5) Å versus 2.7970(5) Å, respectively) because of the difference between the (Br:F) occupancy of each site (i.e., (72%:28%) versus (17%:83%), respectively). For the same reason, the four Nb1–Nb2 bonds bridged by *L*1 are longer than the four others bridged by *L*4 (2.8545(5) Å versus 2.7967(5) Å, respectively) with the following (Br:F) occupancies: (72%:28%) versus (1.7%:98.3%), respectively. Despite the distortion of the Nb_6 cluster in $Cs_2Nb_6Br_5F_{12}$, it is noteworthy that the average Nb-Nb interatomic distance is very close to that reported in $Na_2Nb_7Br_4F_{17}$ (2.8232(5) Å against 2.814(1) Å (9)). Let us recall that the Nb_6 cluster in the latter compound exhibits an ideal $m\text{-}\bar{3}m$ local symmetry. As a matter of fact, the chains of units in $Cs_2Nb_6Br_5F_{12}$ are not perfectly linear even though the Nb–F^{a-a}–Nb bridges are linear. Indeed, the angle between the Nb2–Nb2 direction and the [1 1 0] or [$\bar{1}$ 1 0] directions of propagation of the chains is equal to 2.5°. This point can be understood if one takes into account the aforementioned inhomogeneous distribution of bromine and fluorine on the inner ligand sites. As a consequence, the linear Nb–F^{a-a}–Nb bridges form a staircase arrangement (Fig. 3). The angle between one step of the latter arrangement and the [1 1 0] direction is equal to 2.4°, while the angle between the normal of the $(Nb1)_4$ rectangle and the [1 1 0] direction is equal to 4.1°.

It turns out that the units of $Cs_2Nb_6Br_5F_{12}$ and those of $Ba_2Zr_6Cl_{17}$(B) (10) exhibit the same developed formula, i.e., $M_6X^{i}_{12}X^{a-a}_{2/2}X^{a}_{4}$. Moreover, in both cases, the M–X^{a-a}–M intercluster connections are linear. However, in $Ba_2Zr_6Cl_{17}$(B), the pseudo four-fold axis of the Zr cluster is merged with the Zr–Cl^{a-a} bond leading to a linear arrangement of the successive Zr–Cl^{a-a}–Zr bridges. This feature is explained by the fact that the Zr_6 cluster is not subjected to a significant distortion because it is bonded to only one kind of ligand, in contrast to what occurs in $Cs_2Nb_6Br_5F_{12}$. On the other hand, no obvious structural relationship can be evidenced between $Cs_2Nb_6Br_5F_{12}$ and Nb_6F_{15} (5)—in which the four-fold axis is merged with the Nb–F^{a-a} bond,

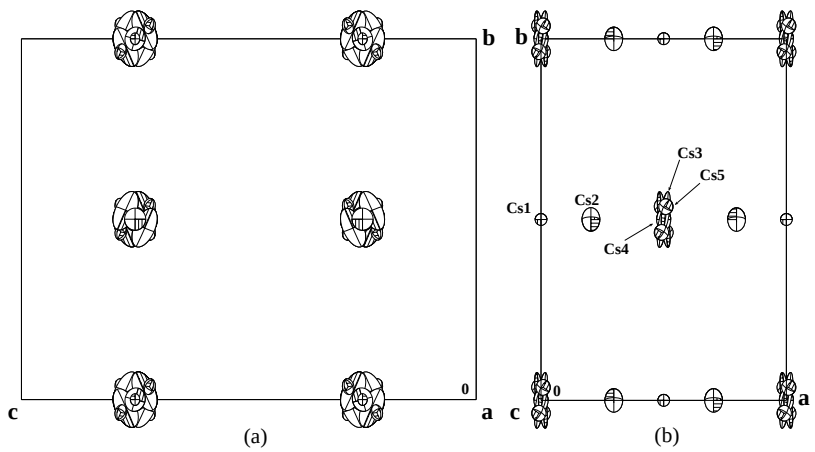

FIG. 4. Projection of the positions statistically occupied by cesium cations in the channels along (a) the [1 0 0] direction and (b) the [0 0 1] direction. Displacement ellipsoids are shown at the 50% probability level.

while the structure of $Ba_2Zr_6Cl_{17}$(B) is related to that of the latter fluoride by a breaking of the apical–apical bridges in two directions together with a twist of the clusters of about 20° with regard to the four-fold axis. In Nb_6F_{15} and $Ba_2Zr_6Cl_{17}$(B), the cluster chains are linear and parallel in the whole direct space. In contrast to the previously discussed structures, in $NaMo_6Cl_8^iCl_{2/2}^{a-a}Cl_4^a$ (11, 12) for which the Mo_6 cluster is bonded to eight face-capping chlorine atoms, the Mo–Cl^{a-a}–Mo bridges are bent as always observed in molybdenum halides and chalcohalides. The value of the VEC (valence electron count) per cluster in the zirconium (10) and the molybdenum (11, 12) compounds—14 and 24, respectively—corresponds to nonmagnetic compounds. In contrast, the VEC of the cluster in $Cs_2Nb_6Br_5F_{12}$ is calculated to be 15. Hitherto, no niobium bromide containing Nb_6 clusters with 15 electrons has been isolated while $Cs_2Nb_6Br_5F_{12}$ constitutes the second example after $Nb_6Br_8F_7$ of a fluorobromide containing Nb_6 clusters displaying 15 electrons per cluster. Such a stabilization may be attributed to the fact that Nb–Nb bond lengths are shorter in the latter fluorobromides than those found in niobium bromides with 16 electrons per Nb_6 cluster (e.g., 2.954(1) and 2.970(1) Å for $CsErNb_6Br_{18}$ and $Cs_2EuNb_6Br_{18}$, respectively (15)). This observation cannot be attributable to the decrease of the VEC value, which would have the reverse effect, because of a depopulation of the HOMO level that is mainly metal–metal bonding (16). Unfortunately, the presence of Cs_2NbF_6 as an impurity in the final product prevents us from studying the magnetic properties of the title compound.

ACKNOWLEDGMENTS

We thank the "Centre de Diffractométrie de l'Université de Rennes 1" for the data collection on the Nonius KappaCCD X-ray diffractometer. In particular, the useful advice of Dr. T. Roisnel is gratefully acknowledged. We are also indebted to C. Derouet for his technical help and to "Fondation Langlois" for its financial support.

REFERENCES

1. C. Perrin, S. Cordier, S. Ihmaïne, and M. Sergent, *J. Alloys Comp.* **229,** 123 (1995).
2. B. Baján and H.-J. Meyer, *Z. Anorg. Allg. Chem.* **623,** 791 (1997).
3. M. E. Sägebarth, A. Simon, H. Imoto, W. Weppner, and G. Kliche, *Z. Anorg. Allg. Chem.* **621,** 1589 (1995).
4. H. Schäfer, H.-G. v. Schnering, K. J. Niehus, and H. G. Nieder-Vahrenholz, *J. Less Common Met.* **9,** 95 (1965).
5. H. Schäfer and H.-G. Schnering, *Angew. Chem.* **76,** 833 (1964).
6. S. Cordier, O. Hernandez, and C. Perrin, *J. Fluorine Chem.* **107,** 205 (2001).
7. S. Cordier and A. Simon, *Solid State Sci.* **1**(4), 199 (1999).
8. L. Le Polles, S. Cordier, C. Perrin, and M. Sergent, *C. R. Acad. Sci. Paris, Ser. II c*, **2,** 661 (1999).
9. S. Cordier, O. Hernandez, and C. Perrin, *J. Solid State Chem.* **158,** 327 (2001).
10. J. Zhang and J. D. Corbett, *J. Less Common Met.* **156,** 49 (1989).
11. M. Potel, C. Perrin, A. Perrin, and M. Sergent, *Mater. Res. Bull.* **21,** 1239 (1986).
12. S. Böchen and H.-L. Keller, *Z. Kristallogr.* **196,** 159 (1991).
13. J. Chassaing, M. B. de Bournonville, D. Bizot, and M. Quarton, *Eur. J. Solid State Inorg Chem.* **28,** 441 (1991).
14. A. Broll, A. Simon, H.-G. v. Schnering, and H. Schäfer, *Z. Anorg. Allg. Chem.* **367,** 1 (1969).
15. S. Cordier, C. Perrin, and M. Sergent, *Z. Anorg. Allg. Chem.* **619,** 621 (1996).
16. F. Ogliaro, S. Cordier, J.-F. Halet, C. Perrin, J.-Y. Saillard, and M. Sergent, *Inorg. Chem.* **37,** 6199 (1998).
17. Nonius, "COLLECT, DENZO, SCALEPACK, SORTAV: KappaCCD Program Package." Nonius B.V., Delft, The Netherlands, 2000.
18. Z. Otwinowski and W. Minor, *in* "Processing of X-ray Diffraction Data Collected in Oscillation Mode," Methods in Enzymology, Vol. 276: Macromolecular Crystallography, part A, pp. 307–326. (C. W. Carter, Jr., and R. M. Sweet, Eds.), Academic Press, New York, 1997.
19. R. H. Blessing, *Acta Crystallogr. A* **51,** 33 (1995).
20. G. Cascarano, A. Altomare, C. Giacovazzo, A. Guagliardi, A. G. G. Moliterni, D. Siliqi, M. C. Burla, G. Polidori, and M. Camalli, *Acta Crystallogr. A* **52,** C-79 (1996).
21. D. J. Watkin, C. K. Prout, J. R. Carruthers, and P. W. Betteridge, "CRYSTALS," Issue 11. Chemical Crystallography Laboratory, University of Oxford, Oxford, 1999.
22. R. P. Shannon, *Acta Crystallogr. A* **32,** 751 (1976).
23. J. R. Carruthers and D. J. Watkin, *Acta Crystallogr. A* **35,** 698 (1979).
24. A. C. Larson, *in* "Crystallographic Computing" (F. R. Ahmed, Ed.), p. 291. Munksgaard, Copenhagen, 1970.